Trans. of the Korean Hydrogen and New Energy Society(2013. 6), Vol. 24, No. 3, pp. 237~241
DOI: http://dx.doi.org/10.7316/KHNES.2013.24.3.237

미세조직 정량 분석을 통한 고체산화물 연료전지용 NiO-YSZ 연료극 전기전도도 예측

완디 와휴디[1,2] · 빌랄 아메드[1,2] · 이승복[1,2†] · 송락현[1,2] · 이종원[1,2] · 임탁형[2] · 박석주[2]
[1]과학기술연합대학원 신에너지학과, [2]한국에너지기술연구원 수소연료전지연구단

Quantitative Microstructure Analysis to Predict Electrical Property of NiO-YSZ Anode Support for SOFCs

WANDI WAHYUDI[1,2], BILAL AHMED[1,2], SEUNG-BOK LEE[1,2†], RAK-HYUN SONG[1,2], JONG-WON LEE[1,2], TAK-HYOUNG LIM[2], SEOK-JOO PARK[2]
[1]Department of Advanced Energy Technology, University of Science and Technology, 217 Gajeong-ro, Yuseong-gu, Daejeon 305-350, Korea
[2]Fuel Cell Research Center, Korea Institute of Energy Research, 102 Gajeong-ro, Yuseong-gu, Daejeon, 305-343, Korea

Abstract >> The correlation between NiO-YSZ microstructure and its electrical property used for SOFC anode was critically evaluated with image processing and direct measurement techniques. These innovative processing techniques were employed to quantify the contiguity of the anode constituent phase. The calculated contiguities were then correlated with electrical conductivity attained from 4-probe DC method. This investigation described that contiguity of nickel oxide phases of an anode has a linear relationship with its electrical conductivity. We observed that the contiguity of NiO increased from 0.18 to 0.50 then electrical conductivity attained was significantly increased from 520 S/cm to 1468 S/cm at 900°C.

Key words : SOFC(고체산화물연료전지), Microstructure(미세구조), Anode(연료극), NiO-YSZ, Contiguity(연결도), PMMA

1. Introduction

Anode support for a solid oxide fuel cells (SOFCs) is desired to have high electrical conductivity and mechanical stability at its operating temperature range (650 – 1000°C)[1-7]. Since in the past couple of years, a great deal of research has been carried out to assess the performance of anodes for solid oxide fuel cells by using a quantitative microstructure analysis through a micrograph generated by either an optical or electron microscopes. This approach is very attractive, since it makes it possible to predict the electrical and mechanical performance of an anode. J-H Lee et al. and K-R Lee et al.[1,2] characterized the relationship between a pure Ni-YSZ anode and its electrical properties by using an image analysis method. In addition, Simwonis et al. and Pihlatie et al.[8,9] success-

†Corresponding author : sblee@kier.re.kr
[접수일 : 2013.6.14 수정일 : 2013.6.28 게재확정일 : 2013.6.30]

fully predicted the coarsening rate of nickel in a nickel based anode through similar technique. However, the previous works have been done by only focusing on properties in bare Ni-YSZ anode without pore-former, so it could not represent the real properties of anode support because practically the microstructure of anode is mainly controlled by using pore former.

In this paper, we studied the relationship between electrical conductivity of an anode support and the contiguity of NiO. For this purpose, we first quantified the contiguity of the anode constituent phases through an image analysis technique. And finally we compared the electrical conductivity which was measured by 4-probe method and the corresponding NiO phase.

2. Experimental

2.1 Sample Preparation

Nickel oxide (J.T. Baker, USA), yttria-stabilized zirconia (Tosoh, Japan) and different size of 10 wt% PMMA (Poly-methyl methacrylate) were ball milled in ethanol for 24 hrs. After drying and sieving, the composite powders were uni-axially pressed at 250 MPa to produce rectangular type specimen (2.8 x 6.1 x 24 mm). The specimen was sintered at 1400℃ in air for 5hrs, and then reduced to Ni-YSZ in a 10% hydrogen +90% nitrogen atmosphere at 700℃ for 14hrs.

2.2 Sample Characterization

Several measurement techniques were employed to characterize the anode support specimen. The electrical conductivity of the specimen was measured with a 4-probe DC technique under reducing atmosphere with a digital source-meter (Keithley 2400, USA). The porosity of the specimen was measured with Mercury Porosimetry.

Viable metallographic procedure was carried out to prepare a mirror-like cross-sectional specimen for microstructural observation with secondary electron microscope. The cross section of the sintered specimen was infiltrated by polymer resin then grinded and polished. The samples were separated from the resin and then thermally etched at the sintering temperature for 10 minutes to highlight the NiO-YSZ grain boundaries. The cross-section of the etched substrates were examined with a high resolution SEM equipped with a back scattered electron detector.

3. Results and Discussions

3.1 Porosity

We measured the open porosity of the anode support specimen after reduction then plot in Table 1. The specimen showed various porosity in the range beteen 20.3% and 35.1% with respect to addition of PMMA. Without PMMA or with addition of small PMMA size, as represented by PMMA-0 and PMMA-1, reduced substrate could not attain the required porosity for the anode SOFC (30-40%)[5-6]. Therefore, although porosity of reduced anode was significantly increased during the reduction process, addition of PMMA is crucial process to reach enough porosity. Anode substrate in PMMA-2 until PMMA-6 show that they have appro-

Table 1. Porosity of anode support after reduction.

Sample	PMMA Size (μm)	Porosity
PMMA-0	-	20.32
PMMA-1	1	24.78
PMMA-2	5	35.05
PMMA-3	7;10;12	34.36
PMMA-4	1.5;2.5;3.0;3.5	37.68
PMMA-5	1.5;3.0;4.0;5.0	38.06
PMMA-6	3.0;4.0;5.0;7.0	40.04

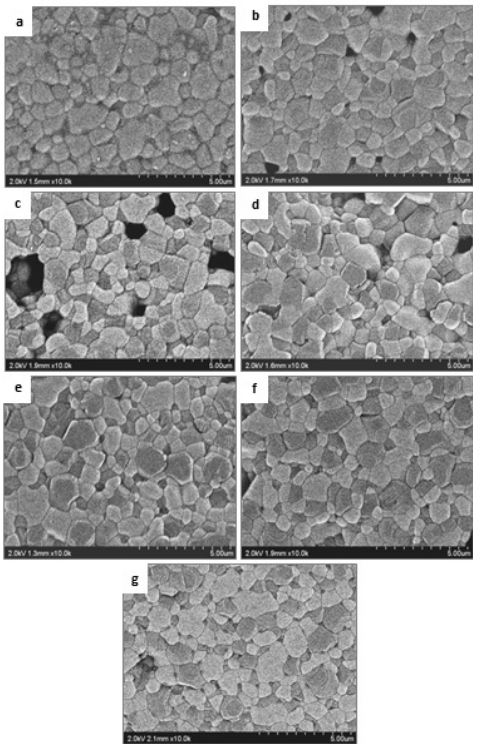

Fig. 1 SEM image on NiO-YSZ composites with various PMMAs: (a) PMMA-0; (b) PMMA-1; (c) PMMA-2; (d) PMMA-3; (e) PMMA-4; (f) PMMA-5; and (g) PMMA-6.

priate porosity after reduction.

3.2 Microstructure

We prepared specimens for cross-sectional view by thermal etching before microstructure observation with SEM. The anode constituent phases (YSZ, nickel oxide, and pores) were distinguished as shown in Fig. 1. The bright area was YSZ, the grey area was nickel oxide, and the black area was pores.

3.3 Electrical Conductivity

Fig. 2 shows the typical temperature dependence of the electrical conductivity of the anode support specimen with respect to types of PMMA. It exhibits

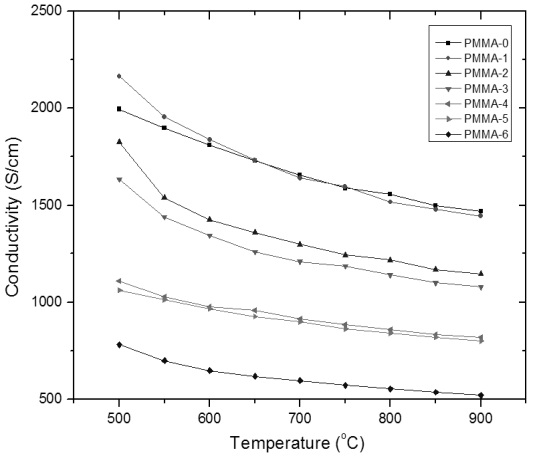

Fig. 2 Temperature dependent electrical conductivity of anode measured in a 10%H2 + 90% N2 atmosphere.

that the electrical conductivities of all the specimens were decreased with the increasing of temperature. This phenomena is similar to the particular behavior of metallic solids. The electrical conductivity of the anode substrate implies that the electrical conduction through the specimen occurs via metallic Ni phase.

The highest electrical conductivity was obtained at PMMA-0, and the lowest electric conductivity was observed at PMMA-6. Furthermore, if we look at the decrease in electrical conductivity of specimen with increasing porosity in Table 1, we realized that the elelctrical conductivity of specimen is strongly influenced by the porosity. Higher porosity might severely diminish the network of the nickel phase, and hence the electrical conductivity will be decreased.

3.4 Quantification of Microstructure

A line-intercept technique was employed to quantify the contiguity of NiO, YSZ, and pore in the anode. We generated multi-parallel lines for each 2D micrograph to determine the interception point of the selected phase on the line. To assure the reliability of the analysis, we generated 150 independent parallel lines with 0.2um line spacing for each digital image.

The following equations[7,8,10] are used to calculate the contiguity between the same phases in a two phase (α, β) composite:

$$N_L = \frac{1}{2} Sv \tag{1}$$

$$C_\alpha = \frac{2Sv_{\alpha\alpha}}{2Sv_{\alpha\alpha} + Sv\alpha\beta} \tag{2}$$

$$C_\alpha = \frac{2NL_{\alpha\alpha}}{2NL_{\alpha\alpha} + NL\alpha\beta} \tag{3}$$

where N_L is the number of contact points in a unit length, S_v is the interfacial area in unit volume, and C_α is the contiguity which represents the degree of contact of the α phase in a two-phase mixture. Based on the equations (1) – (3), a modified equation[6] was proposed for a three-phase composite as follows:

$$C_\alpha = \frac{2NL_{\alpha\alpha}}{2NL_{\alpha\alpha} + NL\alpha\beta + NL\alpha\gamma} \tag{4}$$

where α, β, and γ represents NiO, YSZ, and pores, respectively. By using equation (4), we calculated the three dimensional contiguity of the constituent phase in the NiO-YSZ anode micrograph.

In order to verify the reliability of our imaging interpretation technique, we compared contiguity NiO phases calculated from 5k and 10k SEM magnification. As exhibited in Fig. 3a, the NiO contiguity from the 5k images are well-matched with NiO contiguity from the 10k image magnification. Therefore, we can regard our image analysis technique as a reasonable process to determine quantitative contiguity of NiO phase.

We plotted the calculated contiguity values of NiO and YSZ in Fig. 3b. It is very important to determine the contiguity of the anode substrate constituent phases, because such anode properties as mechanical and electrical properties are strongly influenced by

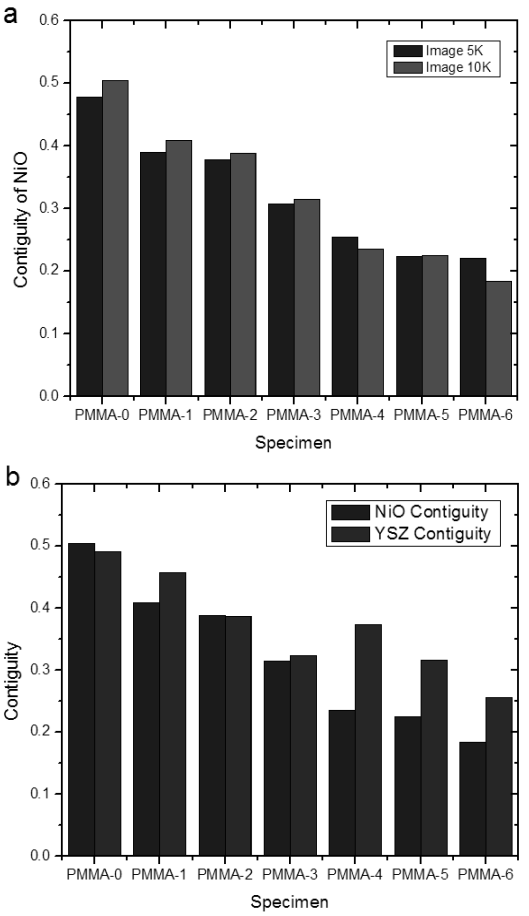

Fig. 3 (a) Comparison of NiO contiguity quantified from 5k and 10k magnification; (b) Contiguity NiO and YSZ phases.

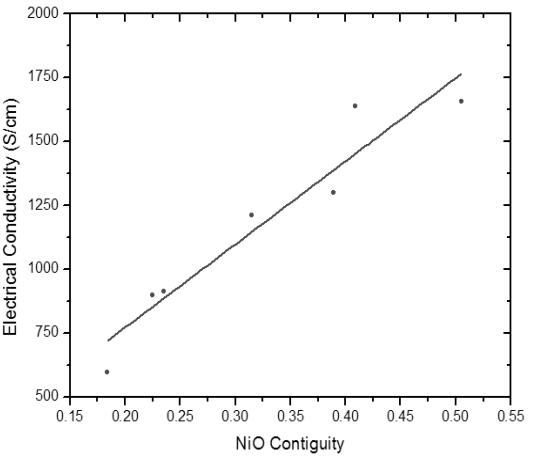

Fig. 4 Electrical conductivity of anode at 700oC as function of NiO contiguity.

the contiguities of corresponding phases.

Fig. 4 exhibits relationship between electrical conductivity of anode support and contiguity of NiO phase. There is linear relation between the two parameters, which enable us to predict electrical conductivity of anode support by image analysis process.

4. Conclusions

In this study, the three anode constituent phases (NiO, YSZ, pore) were controlled with different PMMA. We distinguished the phases by thermal etching process before observation with SEM. Afterward, we quantitatively evaluated microstructure in order to evaluate the relationship between contiguity of NiO and electrical property of anode support specimen.

We observed that there is linear relation between electrical conductivity of anode support and contiguity of NiO phase. This quantitative evaluation technique enable us to predict the properties of anode support in SOFC through its microstructure analysis.

Acknowledgement

This work was supported by the New & Renewable Energy R&D Program under the Ministry of Knowledge Economy (MKE).

References

1. J.-H. Lee, H. Moon, H.-W. Lee, J. Kim, J.-D. Kim, K.-H. Yoon. Quantitative analysis of microstructure and its related electrical property of SOFC anode, Ni-YSZ cermet. Solid State Ionics 148 (2002) 15-26.
2. K.-R. Lee, S.-H. Choi, J. Kim, H.-W. Lee, J.-H. Lee. Viable image analyzing method to characterize the microstructure and the properties of the Ni/YSZ cermet anode of SOFC. Journal of Power Source 140 (2005) 226-234.
3. T. Suzuki, Y. Funahashi, T. Yamaguchi, Y. Fujishiro, M. Awano. Effect of anode microstructure on the performance of micro tubular SOFCs. Solid State Ionics 180 (2008) 546-549.
4. B. R. Roy, N.M. Sammes, T. Suzuki, Y. Funahashi, M. Awano. Mechanical properties of microtubular solid oxide fuel cell anodes. Journal of Power Sources 188 (2009) 220-224.
5. T. Talebi, M.H. Sarrafi, M. Haji, B. Raissi, A. Maghsoudipour. Investigation on microstructures of NiO-YSZ composite and Ni-YSZ cermet for SOFCs. International Journal of Hydrogen Energy 35 (2010) 9440-9447.
6. L. Mingyi, Y. Bo, X. Jingming, C. Jing. Influence of pore formers on physical properties and microstructures of supporting cathodes of solid oxide electrolysis cells. International Journal of Hydrogen Energy 35 (2010) 2670-2674.
7. N. Vivet, S. Chupin, E. Estrade, A. Richard, S. Bonnamy, D. Rochais, E. Bruneton. Effect of Ni content in SOFC Ni-YSZ cermet: A three-dimensional study by FIB-SEM tomography. Journal Power Sources 196 (2011) 9989-9997.
8. D. Simwonis, F. Tietz, D. Stover. Nickel coarsening in annealed Ni-8YSZ anode substrate for solid oxide fuel cells. Solid State Ionics 132 (2000) 241-251.
9. M.H. Pihlatie, A. Kaiser, M. Mogensen, M. Chen. Electrical conductivity of Ni-YSZ composite: Degradation due to Ni particle growth. Solid State Ionics 189 (2011) 82-90.
10. D.-S. Lee, J.-H. Lee, J. Kim, H.-W Lee, H.S. Song. Tuning of the microstructure and electrical properties of SOFC anode via compaction pressure control during forming. Solid State Ionics 166 (2004) 13.